The Use of Texture Descriptors to Improve Automatic Breast Tumor Segmentations in Ultrasound Images

Fabian Torres[1]
Zian Fanti[2]
Ping-Lang Yen[3]
F. Arambula Cosío[4]

[1]PhD Program in Electrical Engineering and Digital Signal Processing, UNAM. Mexico D.F., 04510. fabian.trobles@gmail.com
[2]PhD Program in Computer Science and Engineering, UNAM. Mexico, D.F., 04510. zian.fanti@gmail.com
[3]National Taiwan University, Department of Bio-Industrial Mechatronics Engineering. Taipei, Taiwan. plyen@ntu.edu.tw
[4]Biomedical Imaging Lab, Centro de Ciencias Aplicadas y Desarrollo Tecnológico, UNAM. México, D.F., 04510. fernando.arambula@ccadet.unam.mx

Abstract

Texture descriptors have been widely used in order to improve the results of automatic breast tumor segmentations in ultrasound images. In this work we present a comprehensive evaluation of the ability of different texture descriptors to enhance the contrast between breast tumors and the surrounding tissue in ultrasound images, and how they affect the outcome in automatic segmentations. We evaluated descriptors extracted from the analysis of the histogram, co-occurrence and run-length matrices. The contrast between the tumor region and the surrounding tissue was evaluated using the signal to noise ratio, contrast to noise ratio, histogram intersection and Minkowski-form Distance between the tumor and background histograms. Also the ability to preserve borders was evaluated for each descriptor using the edge preserving index. We have implemented a probabilistic segmentation method in order to evaluate the changes in the accuracy, sensitivity, specificity, and positive and negative predictive values of the method when using different texture descriptors. The results have shown that the Short Run Emphasis of the run-length matrix has better results in the automatic segmentation of breast tumors in ultrasound images with values of 91.96%, 88.58%, 95.99%, 96.34% and 87.58% respectively; also, according with the results, this texture descriptor was the one with higher values in the contrast indexes.

Introduction

Since breast cancer has become the number one cause of death among women around the world, it is very important to have fast and accurate diagnostic methods to improve the prognosis of a patient[1]. Although biopsy is the gold standard for cancer diagnosis, minimal invasion methods for diagnosis are preferred in order to reduce further complications. Mammography and ultrasound are the main two medical imaging modalities for breast tumor screening; several diagnostic methods using ultrasound images have been proposed. Currently, ultrasound is responsible for about one in five of all image based diagnosis[2]. In breast ultrasound images, the malignity of a tumor is estimated by the expert ultrasonographer mainly from its shape, echogenicity (which is an indicator of tumor density) and the internal echo pattern (which describes the texture of the tumor), but the visualization of lesions in ultrasound breast images is a difficult task due to some intrinsic characteristics of the images like speckle, acoustic shadows and blurry edges[3]. Accurate automatic segmentation methods of breast tumors can help the

experts to achieve faster diagnoses, and it's a key stage of fully automatic systems for breast cancer diagnosis using ultrasound images[4].

Texture analysis refers to the characterization of regions in an image according to their texture content, quantifying intuitive qualities described as roughness, smoothness, silkiness and bumpiness[5]. In ultrasound images echo patterns are generally referred as textures[6]. A good breast tumor segmentation method in ultrasound images should take into account texture features in order to differentiate tumors from other objects with similar gray intensities, like glands and acoustic shadows[7]; however, texture analysis in ultrasound images is not an easy task and many metrics have been used to described the echo patterns in breast tumors. Several automatic and semi-automatic segmentation methods using pixel intensity along with texture information have been proposed[7]. Some of these methods use first-order texture descriptors obtained from histogram statistics[7,8], but these descriptors are not able to give a good texture description because they do not take into account the spatial relation between pixels and gray-levels[9]; because of this, other proposed methods use second-order texture descriptors extracted from co-occurrence matrices statistics[10], but the computational cost for computing the co-occurrence matrix is very high and much more demanding while working in per-pixel computation[11]. Other texture descriptors extracted from run-length matrices statistics (which have lower computational cost than co-occurrence matrices) have been used for breast tumor classification in ultrasound images[12].

Texture is a rich source of visual information and there are a number of methods for texture representation, but it is difficult to define the properties than can be used to effectively distinguish textures found in a given image[13]. On the other hand, image enhancement is a key factor to improve the visual appearance of an image and make it more pleasant for human interpretation or more applicable in some special fields such as computer vision, and image processing[14,15]. Because of these, it is important to evaluate which texture descriptor is the one that enhances the contrast of the images the most, and how this improves the outcome of an automatic segmentation method. Except for the work done by Liao et al[6], where they compare the ability of different texture descriptors extracted from co-occurrence matrices statistics to enhance the contrast between the tumor region and the surrounding tissue and how it affects the results of manual and automatic segmentations, there is no related work that evaluates different descriptors extracted from first and second order statistics. In this work we present a comprehensive and extensive evaluation of the effects of texture descriptors (extracted from histogram statistics, co-occurrence matrices statistics and run-length matrices statistics) on the contrast between the tumor region and the surrounding tissue in breast ultrasound images and how this improves the results for an automatic segmentation algorithm. To evaluate the ability of these descriptors to enhance the contrast we obtained different texture images, using per-pixel computation with each texture descriptor, and compare the signal to noise ratio, contrast to noise ratio, histogram intersection and Minkowski-form distance between the tumor region and the surrounding tissue histograms. We also evaluate the ability of these descriptors to improve the segmentation results; we implemented an automatic probabilistic segmentation method based on the work of Madabhushi et al[7] and compare the accuracy, sensitivity, specificity, positive predictive value and negative predictive value of the method when using different texture descriptors. We have found that the short run emphasis of the run-length matrices improves the contrast and the segmentation results previously reported by other authors[6,7].

Materials and Methods

A data base of 30 breast ultrasound images with a lesion were acquired with a GE Healthcare Voluson 73 in the Changhua Christian Hospital, Taiwan. The images were processed in the open source software ITK-SNAP for image enhancement and semi-automatic segmentation supervised by an expert sonographer[16].

Texture Analysis

Here we evaluate different texture descriptors, extracted from histogram statistic, co-occurrence matrices statistics and run-length matrices statistics, in order to find the ability of each descriptor to enhance the contrast between the tumor and the surrounding tissue in breast ultrasound images and how does this reflects in the results of an automatic segmentation algorithm.

First-order texture descriptors are extracted from the original image gray-level values; they do not consider the spatial relationship with neighborhood pixels[17]. The most frequently used first-order descriptors are central moments of the histogram[18]. These descriptors have been used for the segmentation and classification of breast tumors in ultrasound images. Huang et al[8] use the Mean (eq. 1) and Entropy (eq. 2) of the histogram to characterize the texture of breast tumors, also the Kurtosis (eq. 3) and Skewness (eq. 4) of the histogram have been used for tumor classification by Piliouras et al[19]. Another first-order descriptor extracted from the image original values of the image, is the difference of the pixel intensity with the mean of its neighborhood, it is called local variance ($V(i)$, eq. 5) and has been used in automatic segmentation of breast tumors in ultrasound images by Madabhushi et al[7].

$$Mean = \frac{\sum_{x=1}^{M} \sum_{y=1}^{N} I_i(x,y)}{M \times N} \tag{1}$$

$$Entropy = \frac{1}{M \times N} \sum_{x=1}^{M} \sum_{y=1}^{N} I_i(x,y)(-\ln I_i(x,y)) \tag{2}$$

$$Kurtosis = \frac{\sum_{x=1}^{M} \sum_{y=1}^{N} (I_i(x,y) - Mean)^4}{M \times N \times \sigma^4} \tag{3}$$

$$Skewness = \frac{\sum_{x=1}^{M} \sum_{y=1}^{N} (I_i(x,y) - Mean)^3}{M \times N \times \sigma^2} \tag{4}$$

$$V(i) = I_i(x,y) - Mean \tag{5}$$

where I_i is the original image, $M \times N$ is the size of the image and σ is the standard deviation of the gray-level values of I_i.

The gray-level co-occurrence matrix ($GLCM$) describes how frequently two gray-levels (i and j) appear in a window separated by a given distance d and an angle θ[18] (eq. 6).

$$GLCM(i,j|d,\theta) = n_{ij}; d = (d_x, d_y) \tag{6}$$

Second order descriptors computed from the analysis of the co-occurrence matrices have been proposed by Haralick[20]. Some of these descriptors have been used for the segmentation and classification of breast tumors in ultrasound images. Lui et al[10] use the Entropy (eq. 7) and Contrast (eq. 8) of the co-occurrence matrix for breast tumor segmentation. Liao et al[6] evaluated the ability of the Contrast, Homogeneity (eq. 9), Energy (eq. 10) and Variance (eq. 11) of the co-occurrence matrix to enhance the contrast between the tumor and the adjacent tissue in breast ultrasound images, concluding that the Variance is the best texture descriptor of the four to be used in breast tumor contrast enhancement and segmentation in ultrasound images.

$$Entropy_{CM} = \sum_{i,j} GLCM(i,j) \log GLCM(i,j|d,\theta) \qquad (7)$$

$$Contrast = \sum_{i,j} |i-j|^k GLCM(i,j|d,\theta)^l \qquad (8)$$

$$Homogeneity = \sum_{i,j} \frac{GLCM(i,j|d,\theta)}{1+|i-j|} \qquad (9)$$

$$Energy = \sum_{i,j} GLCM(i,j|d,\theta)^2 \qquad (10)$$

$$Variance = \sum_{i,j} (i-e)^2 GLCM(i,j|d,\theta); \quad e = \sum_{i,j} i \cdot GLCM(i,j|d,\theta) \qquad (11)$$

Although co-occurrence matrix based descriptors take into account the spatial relationship between pixels, the computational cost of computing the co-occurrence matrix is very high compared to first-order descriptors[11]. Another method to characterize texture that also takes into account the spatial relationship between pixels, but with lower computational cost than co-occurrence matrices, is based on run-lengths of image gray-levels, were the run-length matrix ($GLRL$) of an image is defined as the number of runs with pixels of equal gray-level i and a given run j inside a maximum distance d and a given angle θ.

$$GLRL(i,j|d,\theta) = n_{ij}; d = (d_x, d_y) \qquad (12)$$

Despite run-length matrix based descriptors have not been widely used as an effective texture classification and analysis method, it has been demonstrated by Tang et al[21] that there is rich texture information contained in this matrices. Galloway[22] proposed five texture descriptors based on the analysis of run-length matrices: short run emphasis (SRE, eq. 13), long run emphasis (LRE, eq. 14), gray-level nonuniformity (GLN, eq. 15), run-length nonuniformity (RLN, eq. 16) and run percentage (RP, eq. 17); these descriptors have been used for the classification of malignancy of breast tumors in ultrasound images[19,23,24].

$$SRE = \frac{1}{n_r} \sum_{i,j} \frac{GLRL(i,j|d,\theta)}{j^2} \qquad (13)$$

$$LRE = \frac{1}{n_r} \sum_{i,j} GLRL(i,j|d,\theta) \cdot j^2 \qquad (14)$$

$$GLN = \frac{1}{n_r} \sum_{i} \left(\sum_{j} GLRL(i,j|d,\theta) \right)^2 \qquad (15)$$

$$RLN = \frac{1}{n_r} \sum_{j} \left(\sum_{i} GLRL(i,j|d,\theta) \right)^2 \qquad (16)$$

$$RP = \frac{n_r}{n_p} \qquad (17)$$

where n_r is the number of total runs and n_p is the number of pixels in the image.

A list of the descriptors evaluated in this work, extracted from first-order, co-occurrence and run-length statistics is show in table 1, along with the works that have used them in order to segment or classify breast tumor in ultrasound images.

Table 1. List of evaluated texture descriptors.

First order	Mean	Huang et al[8]
	Entropy	Huang et al[8]
	Kurtosis	Pilouras et al[19]
	Skewness	Pilouras et al[19]
	Mean Difference	Madabhushi et al[7]
Co-occurrence	Entropy	Liu et al[10]
	Contrast	Liu et al[10]
	Homogeneity	Liao et al[6]
	Energy	Liao et al[6]
	Variance	Liao et al[6]
Run-length	Short Run Emphasis	Lefebvre et al[24]
	Long Run Emphasis	Lefebvre et al[24]
	Gray-Level Nonuniformity	Murmis et al[23]
	Run-length Nonuniformity	Murmis et al[23]

Segmentation Method

Because of inherent artifacts in breast ultrasound images such as speckle and blurry edges, the segmentation of tumors in this kind of images is not an easy task[3]. Several works have been done in order to create semi-automatic and automatic segmentation methods. Based on the literature, these methods can be divided in two groups; thresholding based methods and classifier based methods. The thresholding based methods have low computational cost and usually use only gray-level intensities for segmentation, leading to bad segmentation results since other objects in the image may have similar gray-level intensities[3,8,25]. The classifier based methods are more robust since they use more than one feature for classification, but the implementation and the computational cost increments considerably compared with thresholding based methods[1,7,10,26]; the image features used in a classifier based method should appropriately be selected according to the application, texture information might be suitable for ultrasound images[3].

We have implemented an automatic segmentation method based on the work of Madabhushi et al[7]. This method is based on a region-growing algorithm applied to a probability image instead of an intensity image. A probability image refers to the visual representation of the probability of a pixel to belong to the tumor, with respect to some predefined features; the echogenicity and the internal echo pattern are used as features in this method to compute the pixel probability. Two density probability functions (*pdf*) are obtained from previously segmented images, one for intensity and one for texture.

The intensity *pdf* is obtained from the extraction of the normalized histogram of the tumor region of pre-processed images. Most of the proposed methods for tumor segmentation in breast ultrasound images use a pre-processing step to obtain more homogenous regions and enhance the contrast of the image. For contrast enhancement some works used the stick method[3,25,26], but Madabhushi et al[7] proposed the use of histogram equalization because it is a fast method with good results in tumor enhancement. To obtain more homogenous regions a Gaussian filter was used by Chen et al[3] and a Butterworth filter was used by Madabhushi et al[7], but Abd et al[27] showed that the Gaussian Anisotropic Filter has better results in ultrasound images since it preserves boundaries. Based on this, we

implemented a pre-processing step to obtain a contrast enhanced image using histogram equalization and a Gaussian Anisotropic Filter to obtain more homogenous regions while preserving borders.

To obtain the texture *pdf,* the normalized histogram of the tumor region is extracted from a texture image, obtained by per-pixel computation of the original image using a texture descriptor. Because texture parameters in ultrasound images characterize the acoustic properties of the tissue[24], the texture image was computed from the original image without any pre-processing step to avoid elimination of any texture related information.

After computing the probability image, using the intensity and texture joint probability, extracted from the intensity and texture *pdf*s, the method uses a region growing algorithm on the probability image in order to obtain the region that belongs to the tumor. The seed point of the region is automatically determined by the method using the probability of each pixel, along with spatial information about the potential seed. Usually the ultrasound probe is placed above the region of interest and trying to put the lesion in the center of the image, while the subcutaneous fat, glands and skin are located in the upper part of the image, and acoustic shadows usually are located in the lower part of the image; for this reason, the pixels that are near the central area of the image have more probability of belonging to the tumor according to spatial location. To quantify the probability of each pixel of being the seed of the region growing method $S(x)$, Madabhushi et al[7] proposed a mathematical approach based on eq. 18.

$$S(x) = \frac{I_P(x)N_xY_x}{d_x} \tag{18}$$

where $I_P(x)$ is the joint probability of belonging to the tumor according to texture and intensity features; N_x is the mean of the joint probability in a neighborhood around the pixel; Y_x is the vertical position of the pixel and d_x is the Euclidean distance from the center of the image to the pixel. $S(x)$ is computed for every pixel in the image and the pixel with the highest value is used as the region growing algorithm seed.

To include one pixel t inside the tumor region T it should satisfy two conditions: First, the probability of the pixel $I_p(t)$ should be inside a range of values between the mean of the tumor region probability J_{C_0} by an upper and a lower threshold β_1 and β_2; second, at least one pixel in the immediate neighborhood $N_t(t)$ of the pixel should had been included already in the tumor region; these conditions are shown in eq. 19.

$$t \in T \; if \; \; \beta_1 J_{C_0} \leq I_P(t) \leq \beta_2 J_{C_0} \, and \, T \cap N_t(t) \neq 0 \tag{19}$$

After computing the region growing algorithm the borders of the final region are used as the initialization of a Snake in order to find the final segmentation of the tumor. A complete description of the method can be found in the original work by Madabhushi et al[7]; all the user defined variables of the segmentation method used in this work were extracted from the original works.

Experiments and Results

Contrast enhancement using texture descriptors

Evaluation of contrast enhancement can be done with different indices, but there is no standardized solution for this; therefore, it is important to compute several indices for this purpose in order to have a good contrast enhancement evaluation[28]. To evaluate the ability of the texture descriptors listed in table 1 to enhance the

contrast between the tumor region and the surrounding tissue we used the signal to noise ratio (SNR, eq. 20) and the contrast to noise ratio (CNR, eq. 21), both used by Liao et al[6].

$$SNR = \frac{\mu_{ROI}}{\sigma_{ROI}} \tag{20}$$

$$CNR = \frac{|\mu_{ROI} - \mu_{Background}|}{\sigma_{ROI} + \sigma_{Background}} \tag{21}$$

where μ_{ROI} and $\mu_{Background}$ are the mean brightness values of the tumor region (ROI) and the surrounding tissue (Background) respectively, and σ_{ROI} and $\sigma_{Background}$ are the standard deviations.

In addition to the SNR and CNR we computed the Minkowsky-form Distance (MD, eq. 22) and the histogram intersection (INT, eq. 23) between the ROI and the background regions as similarity measurements between histograms. The MD is often used for computing dissimilarities between histograms[29]. The intersection of the histograms is a useful similarity measurement when the number of pixels is different between images or regions, and also is well suited to deal with scale changes[30].

$$MD(H_{ROI}, H_{Background}) = \left(\sum_i |H_{ROI}(i) - H_{Background}(i)| \right) \tag{22}$$

$$INT(H_{ROI}, H_{Background}) = 1 - \frac{\sum_i \min(H_{ROI}(i), H_{Background}(i))}{\sum_i H_{Background}(i)} \tag{23}$$

where H_{ROI} and $H_{Background}$ are the normalized histograms of the regions.

Along with contrast enhancement, another important aspect to take into account when using texture analysis for image segmentation is the ability of the descriptor to preserve the edges of the structures we want to segment[6]. To evaluate this, we used the edge preservation index (EPI, eq. 24).

$$EPI = \frac{\sum |p_T(i,j) - p_T(i-1, j+1)|}{\sum |p_o(i,j) - p_o(i-1, j+1)|} \tag{24}$$

where $p_T(i,j)$ is the value of the texture image pixel and $p_o(i,j)$ is the value of the original image; the pixel (i,j) is in the edge area, previously segmented in the original image[31].

We compare the SNR, CNR, DM, INT and EPI of the original images with the ones of the texture images obtained using per pixel computation with the descriptors listed in table 1. We also compute these indices for the pre-processing step used in the segmentation algorithm to obtain an intensity image with higher contrast and more homogeneous regions, in order to find out if this step really increases the contrast of the images. Table 2 shows the results for the original image and the pre-processing step, where we can see that the preprocessing step increases all indices except for the SNR and the EPI.

The first-order descriptor that obtained better results enhancing the image contrast was the Mean of the histogram, with higher values of MD, INT and CNR than the original image, however the SNR was lower than in the original image and the ability to preserve borders was low. The results also shows that second-order descriptors based on the co-occurrence matrices are not useful for image enhancement, since none of the descriptors proposed by Haralick[20] are able to enhance the contrast of the image, having lower values in all the evaluation indexes excepting for SNR which was significantly higher in the texture images using co-occurrence based

descriptors; although none of these texture descriptors improve the contrast, the co-occurrence matrix based texture descriptor that obtained the higher values in all indexes was the Homogeneity. Of all the rung-length based texture descriptors the SRE had better results improving the MD, INT, SNR and CNR of the image; this texture descriptor is also the one that increases the MD and INT the most of all the descriptors listed in table 1, making easier the differentiation between regions using their probabilities, since the normalized histogram can be used as the probability density function of belonging to a region[32]. Of all the texture descriptors listed in table 1, the only one that was able to preserve borders was the local variance of the original image gray-values, but this descriptor decreased all the other contrast enhancement indices. The values of the contrast indices for the Mean of the histogram, Homogeneity of the co-occurrence matrices and the SRE of the run-length matrices are shown in table 2; figure 1 shows the images for each descriptor and figure 2 shows the normalized histogram of the tumor region (blue) and background (red) in each image of figure 1.

Table 2. Contrast indices.

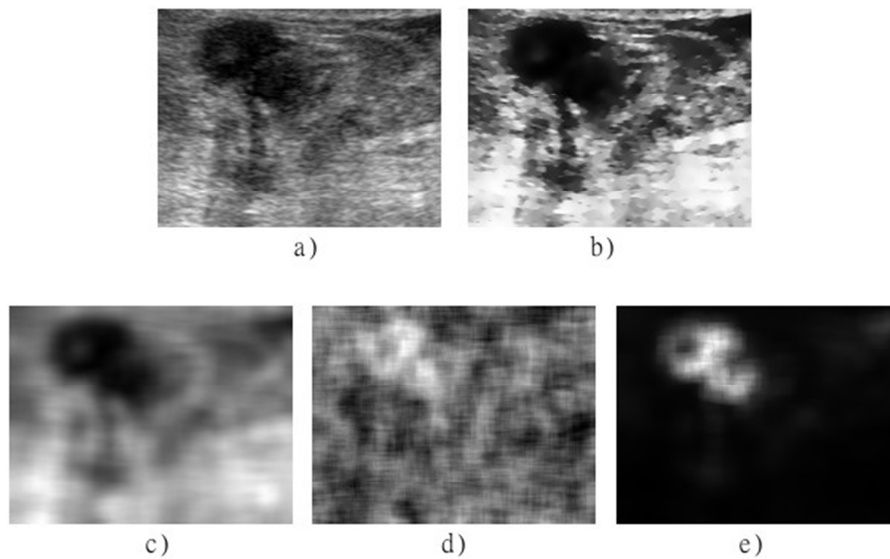| Image	MD	INT	SNR	CNR	EPI
Original	1.4136 ±0.3264	0.2932 ±0.1632	1.7450 ±0.5285	1.0784 ±0.3316	1 ±0
Pre-processed	1.4953 ±0.3132	0.2524 ±0.1566	1.0644 ±0.2333	1.1682 ±0.3610	1.4429 ±0.3702
Mean	1.5460 ±0.3075	0.2270 ±0.1537	1.5996 ±0.3274	1.2495 ±0.3713	0.4048 ±0.1019
Homogeneity	0.8341 ±0.4466	0.5829 ±0.2233	4.0034 ±0.9603	0.5256 ±0.4724	0.5491 ±0.2257
SRE	1.6217 ±0.2944	0.1892 ±0.1472	1.9031 ±0.4847	1.2124 ±0.3924	0.3925 ±0.2319

Figure 1. Textural analysis of breast ultrasound images; a) original ultrasound image, b) pre-processed intensity image, c) mean of the histogram texture image, d) Homogeneity of the co-occurrence matrix texture image, and e) SRE of the run-length matrix texture image.

Segmentation evaluation

We implemented an automatic segmentation method based on the one reported by Madabhushi et al[7], which includes a pre-processing step to obtain an intensity image and a texture image in order to build a probability image to segment the tumor with a region growing algorithm and a Snake. Here we evaluate the results of the segmentation method when using only the original image, only the pre-processed intensity image and using the

pre-processed intensity image along with a texture image obtained with one of the descriptors listed in table 1. To evaluate the segmentation results we used the accuracy (eq. 25), sensitivity (eq. 26), specificity (eq. 27), positive predictive value (PPV, eq. 28) and negative predictive value (NPV, eq. 29)[33].

$$Accuracy = \frac{TP + TN}{TP + TN + FP + FN} \tag{25}$$

$$Sensitivity = \frac{TP}{TP + FN} \tag{26}$$

$$Specificity = \frac{TN}{TN + FP} \tag{27}$$

$$PPV = \frac{TP}{TP + FP} \tag{28}$$

$$NPV = \frac{TN}{TN + FN} \tag{29}$$

where TP, TN, FP and FN are the true positives, true negatives, false positives and false negatives pixels found in the segmentation process. These indices were evaluated for the 30 images using leave-one-out cross-validation.

The accuracy is the ratio of correctly classified pixels (TP and TN) in the entire area of the image[34]. The sensitivity and specificity are often used to complement the evaluation of segmentation algorithms; sensitivity is used to measure how many pixels in the region of interest are correctly segmented, it does not tell anything about how many pixels in the background are going to be segmented as tumor[35]; the specificity measures how many pixels in the background are correctly excluded and does not tell if a tumor pixel is going to be correctly segmented[35]. The positive and negative predictive values are related with sensitivity, specificity and the size of the region, the predictive values will change between images if the tumor region covers a different percentage of the whole image, it is important to take this into account since the size of breast tumors change between patients[36].

Table 3 shows the segmentation results using only the original image without any pre-processing. This table also shows the results of the segmentation using only the intensity image obtained by the pre-processing step; it can be seen that having a more homogeneous image with higher contrast increases the accuracy, specificity and PPV values of the method, but decreases the sensitivity and NPV values by 1.24% and 0.54% respectively. We also evaluated the ability of different texture descriptors to find out which is the one that increases the outcome of the segmentation method the most. Almost all of the first order descriptors enhanced the segmentation results except for the NPV. The first-order descriptor that leads to better segmentation results was the Mean of the histogram, having higher percentage of accuracy, sensitivity, specificity and PPV than using only the intensity of the gray-values of the image, but the NPV value was diminished by 1.22% using this descriptor compared with using only the original image for segmentation. The homogeneity of the co-occurrence matrix was the best descriptor of this type, having higher values of accuracy, sensitivity, specificity and PPV; the NPV was also diminished using this descriptor by 0.54% compared with using the only the original image for segmentation, but a practically the same compared with using only the pre-processed intensity image. The best segmentation results using gray-value intensities and texture information were obtained using the SRE of the run-length matrix, with the highest values in accuracy, sensitivity, specificity, PPV and NPV; although the difference in the NPV vale between the results using this descriptor and using only the original image may not be significant (0.32%), at least this descriptor do not diminished the value as all the other texture descriptors listed in table 1. The results of the segmentation using the best descriptors of each class are also shown in table 3.
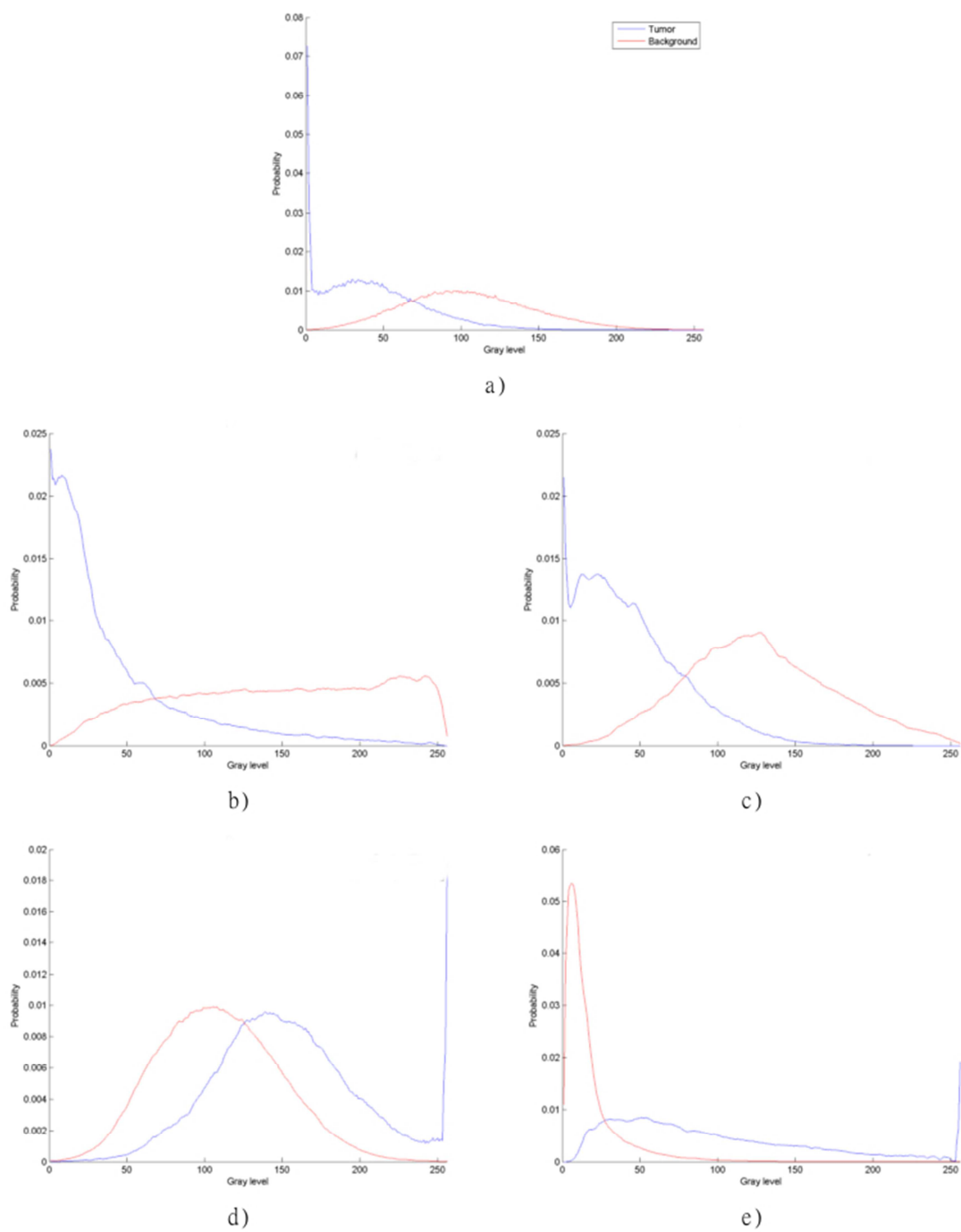
Figure 2. Normalized histograms of textural analysis; a) original ultrasound image, b) pre-processed intensity image, c) mean of the histogram texture image, d) Homogeneity of the co-occurrence matrix texture image, and e) SRE of the run-length matrix texture image.

Table 3. Segmentation results using different texture descriptors

Category	Descriptor	Accuracy	Sensitivity	Specificity	PPV	NPV
Intensity	Original	83.89% ±11.42%	86.51% ±15.63%	87.63% ±14.01%	78.94% ±13.30%	87.26% ±13.23%
Intensity	Pre-processed	87.13% ±10.53%	85.28% ±16.75%	89.52% ±11.64%	85.96% ±11.34%	86.72% ±13.49%
First Order	Mean	90.58% ±08.40%	89.36% ±14.48%	94.24% ±09.56%	94.08% ±10.65%	86.36% ±13.51%
Haralick	Homogeneity	90.60% ±09.48%	88.66% ±10.43%	93.84% ±08.98%	93.40% ±11.02%	86.78% ±13.87%
Run-length	SRE	91.96% ±06.96%	88.58% ±09.83%	95.99% ±06.51%	96.34% ±09.01%	87.58% ±13.21%

Figure 3 shows the segmentation results of a breast tumor in an ultrasound image using different texture descriptors along with the pre-processed intensity image, it also shows the segmentation results obtained using only the original image and only the preprocessed intensity image without any texture information. Table 6 shows the accuracy, sensitivity, specificity, PPV and NPV of the segmented images in figure 3. It can be seen in table 6 that using texture descriptors along with a pre-processed intensity image for breast tumor segmentation can upgrade the results considerably. Although in this image the sensitivity and NPV values were diminished using texture descriptors, the difference may be insignificant (1% and 0.3% respectively) compared with the increase in accuracy, specificity and PPV values (16%, 24% and 34% respectively) using the SRE of the run-length matrix as texture descriptor.

Table 4. Segmentation results for the segmented images shown in figure 4.

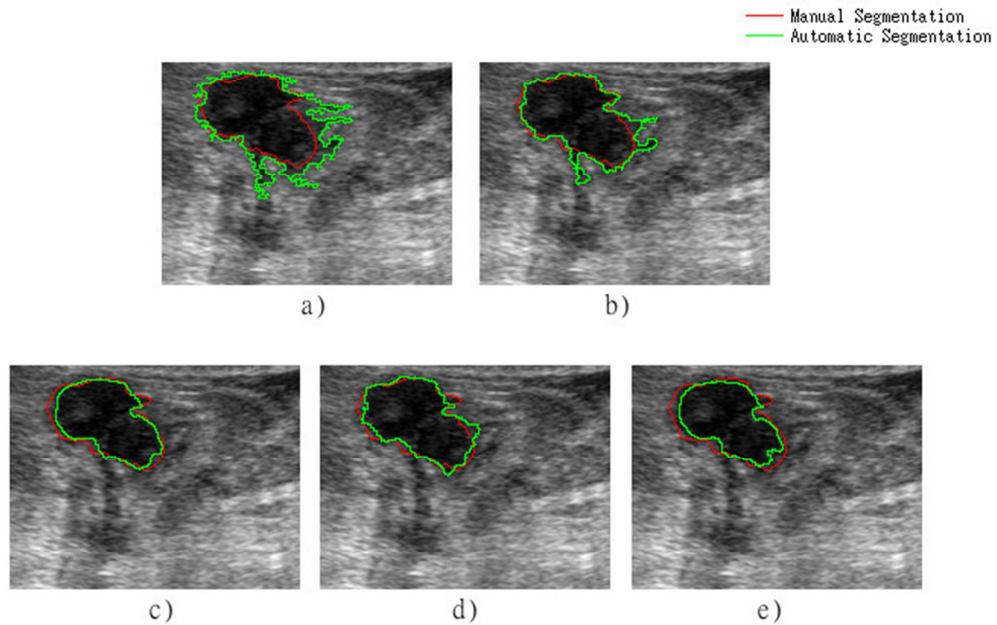| Descriptor	Accuracy	Sensitivity	Specificity	PPV	NPV
Original	82.41%	99.75%	74.03%	64.98%	99.03%
Intensity	91.10%	99.49%	85.14%	82.62%	99.57%
Mean	97.96%	98.50%	97.42%	97.39%	98.52%
Homogeneity	95.97%	98.92%	93.96%	92.96%	98.98%
LRE	98.28%	98.74%	98.84%	98.85%	98.72%

Figure 3. Segmentation of a breast tumor using; a) original image, b) pre-processed intensity image c) mean of the histogram, d) homogeneity of the co-occurrence matrix and e) SRE of the run-length matrix.

Discussion and Conclusion

Texture descriptors have been widely used in breast ultrasound images for tumor segmentation and classification since they help to differentiate structures with similar gray-level intensities from tumors, such as acoustic shadows. In this work we reported a quantitative evaluation of different texture descriptors in order to find out which one is the most effective to enhance the contrast between the tumor and the adjacent tissue and how this affects the outcome of a probabilistic segmentation algorithm like the one proposed by Madabhushi et al[7]. Image quality is a key aspect to consider in ultrasound images since they are affected by many types of artifacts, making hard to an observer to interpret the images and obtain quantitative and qualitative information from them[37].

The ability of different texture descriptors (listed in table 1) to enhance the contrast in the image was evaluated with five indices (MN, INT, SNR, CNR and EPI). It was shown in the results that some of these texture descriptors were able to increase one or more of the used contrast indices. The Mean of the histogram showed good results enhancing the contrast of the image, enhancing almost all the contrast indices except for the SNR and the EPI. It was also shown that none of the co-occurrence based texture descriptors listed in table 1 are good for image enhancement, since none of them was able to increase the value of the contrast indices except for the SNR, but this may not lead to better visualization of the tumor region; looking at eq. 20 a higher SNR value may imply two things, the mean gray-level of the tumor region increased and/or the standard deviation decreased, making the region brighter and/or more homogeneous, but if the contrast between the region and the background is diminished, as with the co-occurrence based texture descriptors, the differentiation of the region of interest is going to be more difficult, since the mean gray-level and the homogeneity of the regions are very similar; figure 4 shows how a breast tumor with high SNR in an ultrasound image does not imply better visualization of the lesion, in this figure the original image has a SNR value of 1.4940 and a CNR value of 1.4882, while the texture image obtained with the correlation of the co-occurrence matrix has a SNR of 3.2322 and a CNR value of 0.0744. The best results of contrast enhancement were obtained using the SRE of the run-length matrices, having the highest values in all indices, except for the EPI which was not increased by any of the texture descriptors listed in table 1 except for the local variance proposed by Madabhushi et al[7]. The proposed pre-processing intensity step, using histogram equalization and an anisotropic filter, showed similar results to the Mean of the histogram, but this pre-processing step was able to preserve the edges of the tumor, meaning that it is a good alternative for breast tumor contrast enhancement in ultrasound images.
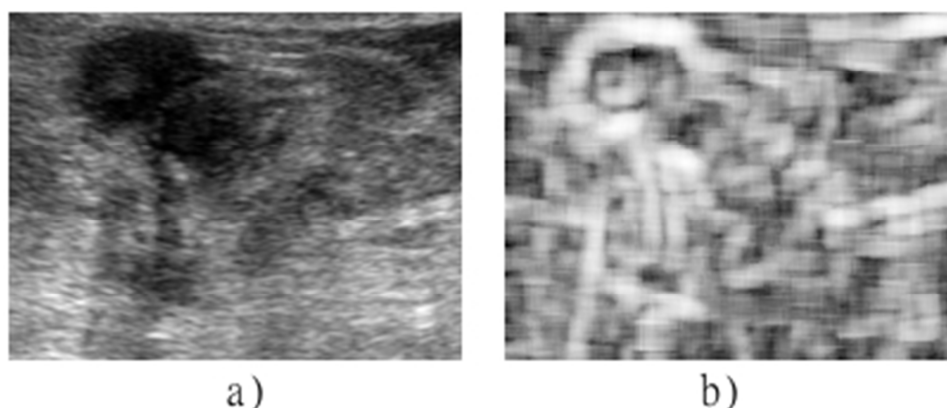

Figure 4. Comparison of lesion visualization with different SNR values a) original image and b) texture image obtained with the correlation of the co-occurrence matrix.

We also evaluated the outcome of a segmentation method when using different texture descriptors; we evaluated the segmentation using five indices (accuracy, sensitivity, specificity, PPV and NPV), and we use a semi-automatic segmentation supervised by a physician as the ground of truth. Table 3 shows that the SRE of the run-length matrices is the texture descriptor of all listed in table 1, that improves the segmentation results the most, having a significant increase in all indices, except for the NPV which was not significantly increased, but the value was not diminished as with all the other texture descriptors; it is important to notice that this texture descriptor was also the one that showed the best contrast enhancement results, increasing the MD and decreasing the Intersection between histograms significantly, making easier to differentiate between regions when using the normalized histogram as a probability function. Although the Mean of the histogram do not lead to the best segmentation results, it also showed good contrast enhancement and segmentation results, as can be seen in table 2 and 3; this means that this texture descriptor may be used instead of the SRE of the run-length matrix for image enhancement and segmentation when time is an important factor, since first-order descriptors have lower computational cost than higher order descriptors[19]. The segmentation results reported in this work showed that texture features provide useful information that helps to distinguish between tumors and the surrounding tissue in breast ultrasound images, table 3 shows that the homogeneity of the co-occurrence matrix provides some information that may improve the outcome of a probabilistic automatic segmentation method even though this texture descriptor does not enhance the contrast of the image, but it may not be suitable for semi-automatic and manual segmentations since the visualization of the lesion may be diminished using this descriptor as explained before.

Although different texture descriptors provide different information about texture of the lesion, our results show that run-length based texture descriptors lead to the best contrast enhancement and segmentation results; in fact, the results of the segmentation using the SRE of the run-length matrix were significantly better compared with the results reported in the work by Madabhushi et al[7], where they reported 76.07% of TP and 76.06 of TN against 96.34% of TP and 87.58% of TN; also the results were better than the ones reported by Liao et al[6], where they reported 95% of TP and 85% of TN when using the variance of the co-occurrence matrix as texture information for their automatic segmentation method. The SRE of the run-length matrix is an indicative of fineness or higher frequency content in an image region; since a fine texture should contain primarily short runs, the improvement of the segmentation results when using this descriptor is most likely due to its ability to detect differences in spatial frequencies, of the speckle patterns, of the tumor and the surrounding tissue[21].

References

1. Jiao J, Wang Y. Automatic boundary detection in breast ultrasound images based on improved pulse coupled neural network and active contour model. 5th International Conference on Bioinformatics and Biomedical Engineering, iCBBE 2011 [Internet]. 2011. Available from: http://www.scopus.com/inward/record.url?eid=2-s2.0-79960133488&partnerID=40&md5=2fbc2be3a6c29e8afa2686a80a22de7d

2. Halliwell M. A tutorial on ultrasonic physics and imaging techniques. Proc Inst Mech Eng Part H J Eng Med [Internet]. 2010;224(2):127–42. Available from: http://www.scopus.com/inward/record.url?eid=2-s2.0-76849088916&partnerID=40&md5=2e31c49ee5eacb38e9d8eff368395571

3. Chen D-R, Chang R-F, Wu W-J, Moon WK, Wu W-L. 3-D breast ultrasound segmentation using active contour model. Ultrasound Med Biol [Internet]. 2003;29(7):1017–26. Available from: http://www.scopus.com/inward/record.url?eid=2-s2.0-0038104383&partnerID=40&md5=7ce9fd930964c1fa833d59c54cbee0f2

4. Moon WK, Lo C-M, Chen R-T, Shen Y-W, Chang JM, Huang C-S, et al. Tumor detection in automated breast ultrasound images using quantitative tissue clustering. Med Phys [Internet]. 2014;41(4):-. Available from: http://scitation.aip.org/content/aapm/journal/medphys/41/4/10.1118/1.4869264

5. Rajaei A, Dallalzadeh E, Rangarajan L. Segmentation of Pre-processed Medical Images: An Approach Based on Range Filter. Int J Image, Graph Signal Process [Internet]. 2012 Sep 1 [cited 2015 Feb 12];4(9):8. Available from: http://www.mecs-press.org/ijigsp/ijigsp-v4-n9/v4n9-2.html

6. Liao YY, Wu JC, Li CH, Yeh CK. Texture feature analysis for breast ultrasound image enhancement. Ultrason Imaging. 2011;33:264–78.

7. Madabhushi A, Metaxas DN. Combining low-, high-level and empirical domain knowledge for automated segmentation of ultrasonic breast lesions. IEEE Trans Med Imaging [Internet]. 2003;22(2):155–69. Available from: http://www.scopus.com/inward/record.url?eid=2-s2.0-0038398643&partnerID=40&md5=8f3c0cb69868bd81039a7d66c017a20e

8. Huang S-F, Chen Y-C, Woo KM. Neural network analysis applied to tumor segmentation on 3D breast ultrasound images. 2008 5th IEEE International Symposium on Biomedical Imaging: From Nano to Macro, Proceedings, ISBI [Internet]. 2008. p. 1303–6. Available from: http://www.scopus.com/inward/record.url?eid=2-s2.0-51049090141&partnerID=40&md5=fb1a47c542dd589d7e2fb66be1f4d161

9. Bader W, Böhmer S, Van Leeuwen P, Hackmann J, Westhof G, Hatzmann W. Does texture analysis improve breast ultrasound precision? Ultrasound Obstet Gynecol [Internet]. 2000;15(4):311–6. Available from: http://www.scopus.com/inward/record.url?eid=2-s2.0-0034543860&partnerID=40&md5=de959bbf56615fddc3548fa4861e418e

10. Liu B, Cheng HD, Huang J, Tian J, Tang X, Liu J. Fully automatic and segmentation-robust classification of breast tumors based on local texture analysis of ultrasound images. Pattern Recognit [Internet]. 2010;43(1):280–98. Available from: http://www.scopus.com/inward/record.url?eid=2-s2.0-68949159836&partnerID=40&md5=849f4e2d8f796deb81ef01d7be063f00

11. F. Igual R. Mayo THUCAR, M.Ujaldon. Optimizing Co-Occurrence Matrices on Graphics Processors Using Sparse Representations. 9th Int Workshop on State-of-the-Art in Science and Parallel Computing, Trondheim, Norway. 2008.

12. Chen W-M, Chang R-F, Kuo S-J, Chang C-S, Moon WK, Chen S-T, et al. 3-D ultrasound texture classification using run difference matrix. Ultrasound Med Biol [Internet]. 2005;31(6):763–70. Available from: http://www.sciencedirect.com/science/article/pii/S0301562905000542

13. Yassine IS, Belfkih S, Najah S, Zenkouar H. A new method for texture image segmentation. 2010 5th International Symposium On I/V Communications and Mobile Network [Internet]. IEEE; 2010 [cited 2015 Feb 12]. p. 1–4. Available from: http://ieeexplore.ieee.org/lpdocs/epic03/wrapper.htm?arnumber=5656161

14. Lv C, Wang G. Image Contrast Enhancement by Optimal Histogram Matching. J Comput Inf Syst. 2015;3:1163–70.

15. Kaur R. Histogram Equalization Tool : Brightness Preservation and Contrast Enhancement using Segmentation with. Int J Comput Appl. 2015;111(2):11–23.

16. P.-L. Yen R.-H. Fan DCY-JCH-CH. Design and construction of 3D breast tumor phantoms for studying morphological effects on biomechanical properties. Int J Comput Assist Radiol Surg. 2013;8(1):S284–5.

17. Selvarajah S, Kodituwakku SR. Analysis and Comparison of Texture Features for Content Based Image Retrieval. Int J Latest Trends Comput [Internet]. 2011;2(1):108–13. Available from: http://www.ijltc.excelingtech.co.uk/vol2issue1/18-vol2issue1.pdf

18. Aggarwal N, Agrawal RK. First and Second Order Statistics Features for Classification of Magnetic Resonance Brain Images. J Signal Inf Process. 2012;3(May):146–53.

19. Piliouras N, Kalatzis I, Dimitropoulos N, Cavouras D. Development of the cubic least squares mapping linear-kernel support vector machine classifier for improving the characterization of breast lesions on ultrasound. Comput Med Imaging Graph [Internet]. 2004;28(5):247–55. Available from:

http://www.sciencedirect.com/science/article/pii/S0895611104000515

20. Haralick RM. Statistical and structural approaches to texture. Proc IEEE. 1979;67(5):786–804.

21. Tang X. Texture information in run-length matrices. Image Process IEEE Trans. 1998;7(11):1602–9.

22. Galloway MM. Texture analysis using gray level run lengths. Comput Graph Image Process [Internet]. 1975;4(2):172–9. Available from: http://www.sciencedirect.com/science/article/pii/S0146664X75800086

23. Murmis VG, Gisvold JJ, Kinter TM, Greenleaf JF. Texture analysis of ultrasound B-scans to aid diagnosis of cancerous lesions in the breast. Ultrasonics Symposium, 1988 Proceedings, IEEE 1988. 1988. p. 839–42 vol.2.

24. Lefebvre F, Meunier M, Thibault F, Laugier P, Berger G. Computerized ultrasound B-scan characterization of breast nodules. Ultrasound Med Biol [Internet]. 2000;26(9):1421–8. Available from: http://www.sciencedirect.com/science/article/pii/S0301562900003021

25. Chang R-F, Wu W-J, Moon WK, Chen D-R. Automatic ultrasound segmentation and morphology based diagnosis of solid breast tumors. Breast Cancer Res Treat [Internet]. 2005;89(2):179–85. Available from: http://www.scopus.com/inward/record.url?eid=2-s2.0-13844267711&partnerID=40&md5=e041bd7389900373ab3295633ebbfbba

26. Huang Q-H, Lee S-Y, Liu L-Z, Lu M-H, Jin L-W, Li A-H. A robust graph-based segmentation method for breast tumors in ultrasound images. Ultrasonics [Internet]. 2012;52(2):266–75. Available from: http://www.scopus.com/inward/record.url?eid=2-s2.0-81855206603&partnerID=40&md5=64f63b465f4e88b93568bd6afd633289

27. Abd-Elmoniem KZ, Youssef A-BM, Kadah YM. Real-time speckle reduction and coherence enhancement in ultrasound imaging via nonlinear anisotropic diffusion. IEEE Trans Biomed Eng [Internet]. 2002;49(9):997–1014. Available from: http://www.scopus.com/inward/record.url?eid=2-s2.0-0036721081&partnerID=40&md5=d5f5fbf546ad5e4399367f427a718bd0

28. Huang D-S, McGinnity M, Heutte L, Zhang X-P, editors. Advanced Intelligent Computing Theories and Applications [Internet]. Berlin, Heidelberg: Springer Berlin Heidelberg; 2010 [cited 2015 Mar 2]. Available from: http://www.springerlink.com/index/10.1007/978-3-642-14831-6

29. Rubner Y, Tomasi C, Guibas LJ. The Earth Mover's Distance as a Metric for Image Retrieval. Int J Comput Vis [Internet]. Kluwer Academic Publishers; [cited 2015 Feb 24];40(2):99–121. Available from: http://link.springer.com/article/10.1023/A%3A1026543900054

30. Barla A, Odone F, Verri A. Histogram intersection kernel for image classification. Proceedings 2003 International Conference on Image Processing (Cat No03CH37429) [Internet]. IEEE; [cited 2015 Feb 24]. p. III – 513–6. Available from: http://ieeexplore.ieee.org/articleDetails.jsp?arnumber=1247294

31. Han Chumning, Guo Huadong, Wang Changlin. Edge preservation evaluation of digital speckle filters. IEEE International Geoscience and Remote Sensing Symposium [Internet]. IEEE; 2002 [cited 2015 Feb 26]. p. 2471–3. Available from: http://ieeexplore.ieee.org/lpdocs/epic03/wrapper.htm?arnumber=1026581

32. Legg PA, Rosin PL, Marshall D, Morgan JE. Improving accuracy and efficiency of mutual information for multi-modal retinal image registration using adaptive probability density estimation. Comput Med Imaging Graph [Internet]. 2013 Jan [cited 2015 Apr 22];37(7-8):597–606. Available from: http://www.sciencedirect.com/science/article/pii/S0895611113001377

33. Chen Q, Liu Q. Textural feature analysis for ultrasound breast tumor images. 2010 4th International Conference on Bioinformatics and Biomedical Engineering, iCBBE 2010 [Internet]. 2010. Available from: http://www.scopus.com/inward/record.url?eid=2-s2.0-77956141441&partnerID=40&md5=fd2549dfd1a9fe290927e5be405faa1f

34. Byrd K, Zeng J, Chouikha M. An assessed digital mammography segmentation algorithm used for content-based image retrieval. 2006 8th international Conference on Signal Processing [Internet]. IEEE; 2006 [cited 2015 May 6]. Available from: http://www.scopus.com/inward/record.url?eid=2-s2.0-34249323051&partnerID=tZOtx3y1

35. Parikh R, Mathai A, Parikh S, Sekhar GC, Thomas R. Understanding and using sensitivity, specificity and predictive values. Indian J Ophthalmol [Internet]. 2008;56(1):45–50. Available from: http://www.scopus.com/inward/record.url?eid=2-s2.0-38149096396&partnerID=tZOtx3y1

36. Akobeng AK. Understanding diagnostic tests 1: sensitivity, specificity and predictive values. Acta Paediatr [Internet]. 2007 Mar [cited 2015 Feb 26];96(3):338–41. Available from: http://www.ncbi.nlm.nih.gov/pubmed/17407452

37. Contreras Ortiz SH, Chiu T, Fox MD. Ultrasound image enhancement: A review. Biomed Signal Process Control [Internet]. 2012 Sep [cited 2015 Apr 15];7(5):419–28. Available from: http://www.sciencedirect.com/science/article/pii/S1746809412000183